Environ. Sci. Technol. **2001**, *35,* 427−433

Rapid Prediction of Long-Term Rates of Contaminant Desorption from Soils and Sediments

MARTIN D. JOHNSON AND WALTER J. WEBER, JR.*

Environmental and Water Resources Engineering, Department of Civil and Environmental Engineering, The University of Michigan, Ann Arbor, Michigan 48109-2125

A method using heated and superheated (subcritical) water is described for rapid prediction of long-term desorption rates from contaminated geosorbents. Rates of contaminant release are measured at temperatures between 75 and 150 °C using a dynamic water desorption technique. The subcritical desorption rate data are then modeled to calculate apparent activation energies, and these activation energies are used to predict desorption behaviors at any desired ambient temperature. Predictions of long-term release rates based on this methodology were found to correlate well with experimental 25 °C desorption data measured over periods of up to 640 days, even though the 25 °C desorption rates were observed to vary by up to 2 orders of magnitude for different geosorbent types and initial solid phase contaminant loading levels. Desorption profiles measured under elevated temperature and pressure conditions closely matched those at 25 °C and ambient pressure, but the time scales associated with the high-temperature measurements were up to 3 orders of magnitude lower. The subcritical water technique rapidly estimates rates of desorption-resistant contaminant release as well as those for more labile substances. The practical implications of the methodology are significant because desorption observed under field conditions and ambient temperatures typically proceeds over periods of months or years, while the high temperature experiments used for prediction of such field desorption phenomena can be completed within periods of only hours or days.

Introduction

Rates of desorption associated with the release of hydrophobic organic contaminants (HOCs) from soils and sediments into interstitial waters are typically biphasic in character, with an initial rapid desorption phase that occurs over a few hours or days being followed by an extremely slow desorption process that can take months or years to reach an end point (*1*−*5*). Such slow desorption is frequently the rate-limiting step in biodegradation, bioremediation, and subsurface transport processes (*5*−*11*). A reliable means for rapidly predicting the long-term desorption behavior of HOCs from contaminated soils and sediments would be invaluable for engineers and scientists planning remediation schemes and/or assessing risks associated with alternative remediation end point decisions.

* Corresponding author e-mail: wjwjr@engin.umich.edu; phone: (734)763-2274; fax: (734)763-2275.

Several other methods for rapidly measuring the labile and bioavailable fraction of sorbed HOCs have been proposed. Mild solvent extractions with butanol, propanol, methanol, or ethyl acetate for periods ranging from 5 s to several minutes have been found to approximate trends in contaminant bioavailability measured by microbial degradation or earthworm uptake (*12*−*15*). However, such methods have several marked disadvantages. First, optimal conditions of specific solvent, dilution, degree of agitation, and duration of extraction for predictive purposes vary with each pollutant, type of microorganism, and type of soil or sediment (*6, 12*−*17*), thus generating huge matrixes of operationally defined results. Second, additions of organic solvents can displace HOCs from binding sites, causing desorption processes and associated rates that are different than those occurring in natural aquatic systems. Finally, mild solvent extraction techniques are not useful for predicting the long-term desorption rates associated with the nonlabile or desorption resistant HOC fractions, and it is these fractions that must commonly limit rates of remediation.

Supercritical CO_2 extractions have also been used to estimate the more readily released fractions of sorbed HOCs (*18*). This technique has the advantages that solvent density and diffusivity are easily adjusted with temperature and pressure and that high diffusivities and low surface tensions in such systems accelerate HOC extraction. It has been shown however, at least for phenanthrene, that supercritical CO_2 desorption does not parallel aqueous desorption, possibly because of the swelling of amorphous organic matter matrixes in the CO_2 (*19*). In addition, enthalpies of sorption of solutes such as phenanthrene to typical geosorbents have been found to be significantly greater in supercritical CO_2 systems than in aqueous systems, making extrapolations from one type of extraction system to the other difficult (*20, 21*). Like mild solvent extraction, supercritical CO_2 extraction cannot be used effectively to predict rates for the more slowly desorbing resistant HOC fractions.

Because HOCs desorption occurs principally into aqueous phases in natural systems, it would seem most logical to conduct accelerated desorption experiments in liquid water rather than in nonaqueous solvents. The 15-day (*17*) and/or 21-day (*6*) desorption of HOCs from soils and sediments to aqueous phases containing excess Tenax polymeric resin has in fact been reported to correlate reasonably well to short-term bioavailability. However, the technique does not provide characterization of desorption rates of resistant fractions unless experiments are continued for impractically long (months or years) periods of time. This is again a critical deficiency because it is usually the slowly desorbing HOC fractions that are most difficult to remove. Experiments reported in this paper examine 25 °C desorption processes for such "impractically long time periods" (up to 640 days) in order to establish baselines against which to compare the results of the predictive technique described.

There is a logical theoretical basis for using an activation energy based technique such as that described herein. Mechanisms proposed as potentially responsible for the commonly observed slow desorption of HOCs from soils and sediments include intraorganic matter diffusion (*2, 3, 22, 23*) and hindered pore diffusion (*5, 24*−*30*), both of which can be considered "activated" processes. Diffusion through soil organic matter is analogous to diffusion in polymers, i.e., diffusing molecules must actually penetrate the polymeric matrix (*31*−*33*). Activated pore diffusion can result from either steric hindrance or retardation by sorption to organic phases associated with pore walls. Desorption from high energy sites

10.1021/es001392c CCC: $20.00
Published on Web 12/15/2000

may also be an important rate limiting step. In condensed polymeric organic matter, HOCs may sorb strongly in molecular sized voids or "holes" (*33*, *34*), while during pore diffusion HOCs are subject to high energy sorption in molecular sized pores (*5*, *29*, *35*, *36*). In either case, desorption rates for such activated processes can be significantly enhanced by increasing temperature. The concept of temperature extrapolations of rate processes is then an obvious extension of the Arrhenius theory. Its potential application for desorption of organic materials from soils has in fact been suggested (*5*, *37*) but not demonstrated.

Materials and Methods

Geosorbents. The natural sorbents used were chosen on the basis of the functional properties of their associated soil/sediment organic matter (SOM). Chelsea soil (particle size <2000 μm), a geologically young topsoil collected near Chelsea, MI, contains SOM (5.62 wt % organic carbon) having extractable humic and fulvic acid organic matter characteristics. Lachine shale (63−180 μm), collected near Alpena, MI, is a geologically older sediment containing SOM (8.27 wt % organic carbon) comprised primarily by type II kerogen. Kerogen, as opposed to the organic matter associated with Chelsea soil, is relatively nonextractable, chemically reduced, and physically condensed (*38*, *39*). Shale is significant in aquifer materials that contain glacial till, such as Wagner soil. Wagner soil (450−500 μm) is a sandy soil with 0.5% (by weight) organic carbon, mostly in the form of intermixed shale particles. Previous publications by Weber and coworkers have characterized the properties and sorption behaviors of the Chelsea soil (*19*−*21*, *40*, *41*), Lachine shale (*42*, *43*), and Wagner soil (*44*, *45*).

Solute. Phenanthrene obtained from Aldrich Chemical Co., Inc. in spectrophotometric-grade was utilized as a probe HOC for the desorption experiments.

Sorption Isotherms. Established bottle-point, fixed-dosage experimental procedures were used for measurements of phenanthrene equilibrium sorption isotherms. Flame-sealed, glass-ampule CMBRs (completely mixed batch reactors) were used to ensure complete mixing and minimize system losses of phenanthrene, which were less than 4% in all cases. Details of the experimental procedures employed have been reported in earlier publications (*41*, *46*). Preliminary investigations showed that a 3-week contact period was sufficient to attain apparent sorption equilibrium for the Chelsea soil, while Lachine shale and Wagner soil required 3-month equilibration periods.

Sorbent Loading for Desorption Experiments. The sorbents were exposed to the probe HOC in 1-L glass bottles filled with buffer solution and a predetermined mass of solid phenanthrene crystals. The buffer solution contained 0.005 M $CaCl_2$ as a mineral constituent, 100 mg/L NaN_3 to control biological activity, and 0.005 g/L $NaHCO_3$ to maintain a pH of 7.0. Before exposure to the probe HOC, the Wagner soil was additionally irradiated using Co-60 with 5 Mrad for 2 h to eliminate microbial activity; the NaN_3 was sufficient to limit biodegradation of phenanthrene in the Chelsea soil and Lachine shale systems. Because phenanthrene sorption capacity decreases in the order Lachine shale > Chelsea soil > Wagner soil, sorbent masses employed for the HOC loadings were 20, 30, and 40 g, respectively. Low and high sorbent loading levels in the various reactors were accomplished by adding enough phenanthrene (predetermined from the sorption isotherms) to give corresponding final aqueous phase equilibrium concentrations of approximately either 20 or 800 μg/L, respectively.

The spiked reactors were mixed end-over-end on a tumbler at 12 rpm for the first month of phenanthrene contact to ensure CMBR conditions, after which the bottles were stored at 25 °C and manually agitated weekly for the remainder of the 3-month aging period. Aqueous phenanthrene concentrations verified that all solid phenanthrene crystals had dissolved within the first 2 weeks of contact, and final solution phase concentrations well below the solubility limit of the solute verified that all phenanthrene was either dissolved in solution or sorbed to the geosorbents; phenanthrene solubility at 25 °C is about 1200 μg/L (*47*). To ensure accurate solid-phase phenanthene concentrations, a mass balance was determined at the end of the aging stage by analysis of aqueous and solid-phase phenanthrene concentrations, the latter by 24-h methanol Soxhlet extractions or 250 °C subcritical water extraction (*48*). The subcritical water extractions proved more effective than methanol Soxhlet extractions. Overall mass balances for all contaminated geosorbents were between 95 and 105%, indicating that experimental losses and microbial degradation were negligible.

Desorption at 25 °C. Rate experiments at 25 °C were conducted in a manner similar to that described above for the sorption isotherm measurements. The CMBRs were flame-sealed glass ampules mixed continuously in a horizontal position on a shaker table. Tenax polymeric resin was added to each reactor to maintain an infinite-dilution condition in solution phase. Several reactors having identical contents were run in parallel for each contaminated sample. At selected times throughout the experiment, a single reactor from each set was opened; the Tenax, aqueous phase, and geosorbent were separated; and the total mass of phenanthrene sorbed to the Tenax phase was analyzed. In this manner, each CMBR was used to generate a single point on a desorption profile. Samples of the aqueous phase were taken for each quenched CMBR to verify that the solution phase phenanthrene concentration was negligible (<1 μg/L). Phenanthrene was extracted from the Tenax beads using hexane, and the phenanthrene concentration in the hexane was determined by HPLC utilizing UV detection. Mass balances for all reported data were within 90−110% of the total added, indicating that system losses (including any attributable to microbial activity) were insignificant.

High-Temperature Desorption. Desorption at 75, 100, and 150 °C was accomplished in a superheated water system similar to that described in an earlier paper (*40*) for extraction of SOM from various geosorbents. To summarize briefly, helium-sparged distilled and deionized water was pumped at a rate of 1.0 mL/min through a preheat coil and a stainless steel sample cell in a GC oven. The hot water containing desorbed phenanthrene exited the oven, passed through a cooling coil, and was depressurized via a series of back pressure regulators. All tubing was 0.0625 in. o.d. by 0.02 in. i.d. stainless steel. Back pressure was not required for the 75 °C extractions because at this temperature water remains in the liquid phase under atmospheric pressure. Back pressures of 5 and 20 atm were applied for the 100 and 150 °C desorptions, respectively, to avoid conversion of liquid water to steam. Repeated experiments at pressures up to 70 atm revealed that applied pressures above those required to keep the water in liquid phase had no effects on phenanthrene desorption rates. Extracted samples were collected sequentially under ambient temperature and pressure conditions in glass vials or jars. All collected effluent was analyzed in each desorption experiment to ensure accurate determination of the total amount of phenanthrene desorbed. Cooling coils and back pressure regulators were flushed constantly with a 1:2 methanol:water mixture (volume ratio) using a second HPLC pump and a mixing "T" at the oven exit.

The high-temperature desorption experiments required 1.0, 0.5, and 0.1 g of Wagner soil, Chelsea soil, and Lachine shale, respectively. Different masses of sorbent were again necessary because of the differences between the phenanthrene uptake capacities of the three sorbents. Experiments

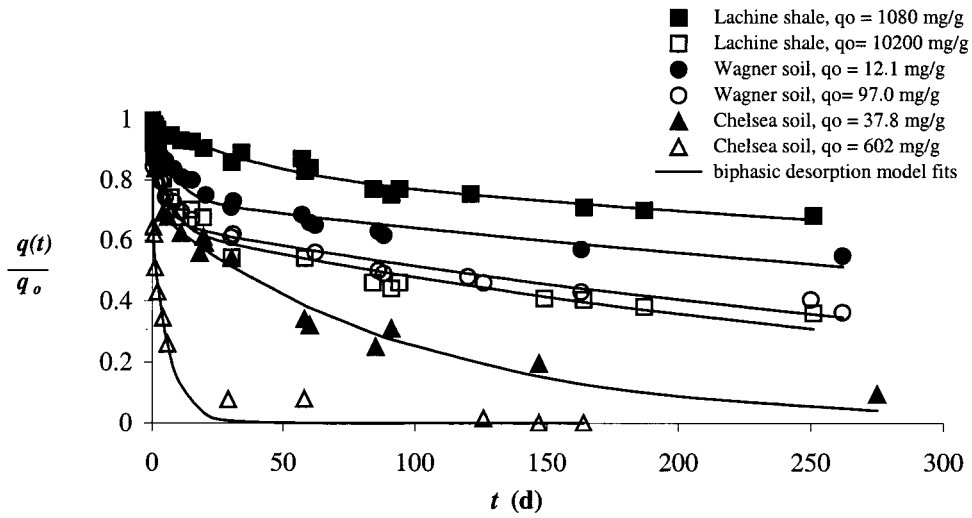

FIGURE 1. Phenanthrene desorption rate profiles for different geosorbents and initial solid-phase loadings at 25 °C under infinite dilution conditions in CMBRs.

were designed so that aqueous phase effluent concentrations were more than 1 order of magnitude lower than phenanthrene solubility during the initial rapid desorption phase, and more than 2 orders of magnitude lower during the slowly desorbing phase. There was therefore always a strong driving force for desorption that minimized potential readsorption phenomena.

Superheated water desorption at 150 °C results in the removal of a small fraction of soil organic carbon from the sorbents, which may in turn enhance phenanthrene desorption by increasing the apparent solubility of phenanthrene in the aqueous solution during the rapid desorption phase. Maximum aqueous phase soil organic carbon concentrations of 1.7, 2.8, and 47 mg/L for the Wagner soil, Lachine shale, and Chelsea soil, respectively, occurred during the first 5−10 min of the high temperature desorption and subsequently declined to negligible amounts over longer desorption times. Desorption at 75 or 100 °C removed order of magnitude lower amounts of soil organic carbon. However, it was in all cases deemed appropriate to treat any increases in phenanthrene solubility due to dissolved organic matter as less significant than increases in phenanthrene solubility at the corresponding elevated temperatures.

Each desorption experiment was terminated with a 1-h, 250 °C, 100 atm step to remove any remaining phenanthrene and obtain a complete mass balance. Mass balances for all reported phenanthrene desorption data were within 90−105% of the total added. Batch desorption experiments utilizing excess Tenax might also be run at elevated temperatures to serve the same purpose as these column experiments, but temperatures would have to be limited to less than 100 °C unless pressure vessels are used.

Results and Discussion

It is possible as noted earlier to use either diffusion models (*3*, *25*, *28*−*30*, *49*) or multi-compartment first-order models (*26*, *37*, *50*−*53*) for describing HOC desorption rates. Here we apply a three-parameter, two-compartment, first-order rate equation that assumes a slowly desorbing fraction, ϕ_s, and a rapidly desorbing fraction, $1 - \phi_s$:

$$\frac{q(t)}{q_o} = \phi_s \exp(-k_s t) + (1 - \phi_s) \exp(-k_r t) \qquad (1)$$

where $q(t)$ is the solid-phase sorbate concentration at a given time, q_o is the initial solid-phase sorbate concentration, and k_s and k_r are apparent first-order rate constants for the slowly and rapidly desorbing fractions, respectively. The model was fit to desorption rate data using the Levenberg−Marquardt nonlinear regression technique with software designed to minimize the sum of squared residuals (SAS Institute, Inc., Cary, NC). The 25 °C desorption data are described using several other rate models in a companion publication in which it is shown (*54*) that the biphasic first-order model, which is attractive because of its simplicity, was found adequate for samples having similarly wide ranges of desorption characteristics.

We investigated the temperature dependence of the rate of release of the slowly desorbing phenanthrene fraction, a dependence that can be described in terms of the Arrhenius relationship

$$k_s(T) = k_o \exp\left(-\frac{E_{app,d}}{RT}\right) \qquad (2)$$

in which k_o is the Arrhenius preexponential factor, $E_{app,d}$ is the apparent activation energy of the slow desorption process, R is the universal gas constant, and T is temperature in degrees Kelvin. If the activation energy associated with a process and a value of the rate constant at some specific temperature are known, a rate constant at a different temperature can be calculated using the Arrhenius model in the form

$$\frac{k_s(T_2)}{k_s(T_1)} = \exp\left(\frac{E_{app,d}(T_2 - T_1)}{RT_1T_2}\right) \qquad (3)$$

The Freundlich isotherm model was used for analysis of the equilibrium sorption data, i.e.

$$q_e = K_F C_e^{\,n} \qquad (4)$$

where q_e is the equilibrium solid-phase concentration of sorbate and C_e is its corresponding equilibrium solid-phase concentration. The parameter K_F is the Freundlich unit-capacity coefficient, and n is a joint measure of the relative magnitude and diversity of energies associated with a particular sorption process (*55*). The Freundlich isotherm is theoretically related to one consisting of multiple Langmuir terms and is thus a logical choice for heterogeneous sorbents (*44*, *55*).

Desorption rate data and model fits are shown in Figure 1, and the corresponding model parameters are listed in Table 1. Trends in desorption parameters as a function of sorbent type and initial phenanthrene solid-phase concentration are

TABLE 1. Phenanthrene Desorption Rate Parameters as Functions of Sorbent Type and Initial Solute Loading Level

		first-order biphasic desorption model parameters		
sorbent	q_o[a] (μg/g)	ϕ_s	k_s (day^{-1}) $\times$ 10^3	k_r (day^{-1})
Lachine	1080	0.829 $\pm$ 0.090[b]	0.859 $\pm$ 0.598	0.0289 $\pm$ 0.0216
Lachine	10200	0.640 $\pm$ 0.071	2.92 $\pm$ 1.03	0.180 $\pm$ 0.099
Wagner	12.1	0.736 $\pm$ 0.040	1.38 $\pm$ 0.53	0.134 $\pm$ 0.055
Wagner	97.0	0.690 $\pm$ 0.043	3.01 $\pm$ 0.73	0.362 $\pm$ 0.147
Chelsea	37.5	0.706 $\pm$ 0.051	10.7 $\pm$ 2.0	0.598 $\pm$ 0.371
Chelsea	602	0.616 $\pm$ 0.110	148 $\pm$ 140	7.30 $\pm$ 5.0

[a] Initial solid-phase solute concentration (μg of phenanthrene/g of sorbent). [b] 95% confidence intervals.

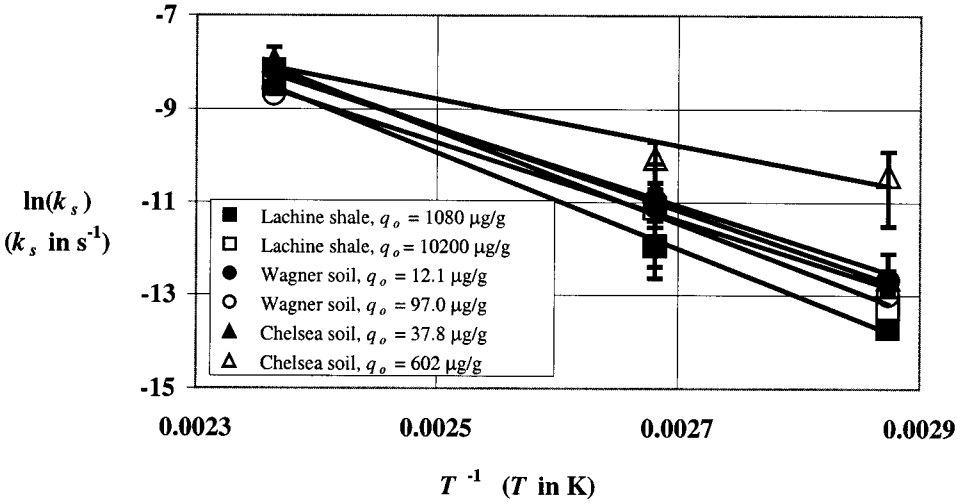

FIGURE 2. Arrhenius plots of first-order rate constants to determine activation energies for slow desorption.

discussed in a companion paper (*54*); here we briefly make two principal observations. First, desorption rates and extents are strong functions of geosorbent type, and we attribute this in large part to the different nature of natural organic matter that each contains. It was an intentional part of the experimental design to select and prepare sorbents exhibiting a broad spectrum of desorption characteristics with respect to both rate parameters and resistant fractions. The results agree with the hypothesis on our part that geosorbents containing primarily humic type organic matter will allow more labile (faster and more complete) desorption than those containing primarily kerogen-like organic matter. Second, for all three sorbent types, rates and extents of desorption increase with higher initial solid-phase solute loading levels. This may be attributable to the distribution of sorption site energies associated with SOM (*44*) or to non-Fickian diffusion (i.e., concentration-dependent diffusivities) through polymeric SOM matrixes. The latter effect is analogous to that which occurs for solute diffusion through glassy polymers (*33*, *43*, *56*).

The implications of the observed effects of initial loading levels are significant, highlighting a critical facet of the need in remediation practice for a predictive methodology such as that presented here. Given the evidence that HOC desorption rates depend on sorbed-phase concentrations reached in earlier contamination events, predictions based solely on the native properties of the geosorbent are insufficient. Conversely, if the precepts set forth here are correct, relatively simple hot water desorption experiments coupled with calculations of apparent activation energies of desorption for specific samples at specific levels of contamination may allow accurate predictions of slow long-term desorption rates to be expected in each specific case.

Activation Energies. Arrhenius-type plots of ln(k_s) versus 1/T for the six samples are shown in Figure 2, confirming the applicability of the Arrhenius relationship for describing the temperature dependence of the desorption process, thus allowing calculation of activation energies from the respective slopes ($-E_a/R$) of the resulting straight lines. Analysis of the phenanthrene desorptions measured at 75, 100, and 150 °C, resulted in determinations of the apparent activation energies of desorption listed in Table 2. Values of $E_{app,d}$ ranging from about 40 to 80 kJ/mol are consistent with those for diffusion in polymers, which average approximately 60 kJ/mol but can exceed 100 kJ/mol for glassy or highly cross-linked polymeric matrixes (*26*, *31*, *32*, *56*–*58*). Sterically hindered pore diffusion typically has lower activation energies, i.e., 10–50 kJ/mol (*36*, *37*, *57*, *59*–*61*). Other studies of HOC desorption from soils and sediments have yielded apparent activation energy values similar to those presented in Table 2; specifically, 60–70 kJ/mol for desorption of chlorobenzenes, PCBs, and PAHs from sediments (*37*) and 66 kJ/mol for EDB desorption from soil (*5*).

TABLE 2. Temperature Effects on Solute Desorption Rates

sorbent	q_o (μg/g)	$E_{app,d}$[a] (kJ/mol)	k_s (75 °C)/k_s (25 °C)[b]
Lachine	1080	85.8 $\pm$ 9.9	145
Lachine	10200	82.6 $\pm$ 10.1	120
Wagner	12.1	74.1 $\pm$ 4.4	73
Wagner	97.0	69.3 $\pm$ 18.1	56
Chelsea	37.8	69.4 $\pm$ 13.1	56
Chelsea	602	41.3 $\pm$ 25.5	11

[a] Activation energy of phenanthrene desorption determined from rate data at 75, 100, and 150 °C. [b] Predicted from $E_{app,d}$ and eq 3.

The data in Figure 2 and Table 2 illustrate clearly that the apparent activation energies of such desorption processes are strong functions of sorbent organic matter characteristics and initial contaminant loading level. Desorption activation energies are lower for the Chelsea soil, which contains largely

humic soil organic matter, than they are for the kerogen-containing Wagner soil and Lachine shale. Further, desorption activation energies increase with decreasing initial solid-phase solute concentration. Assuming that there is a distribution of sorption site energies associated with SOM (*44*), the higher energy sites may be preferentially occupied. Thus, at lower loading levels a higher percentage of sorbate molecules are sorbed to higher energy sites, presumably resulting in higher associated desorption activation energies.

It should be noted that temperature itself may cause soil organic matter to become more rubbery as glass transition temperatures are approached or exceeded (*62*). However, when the 25 °C desorption rate constants for the present studies are included in the Arrhenius plot of Figure 2, a strong linear relationship between $\ln(k_s)$ and T^{-1} still exists, verifying that the apparent activation energies of desorption determined from the superheated water experiments remained essentially constant over the broader temperature range studied in the desorption experiments.

Rapid Prediction of Long-Term Desorption Rates. The experimentally determined activation energies were used in eq 3 to predict ratios of phenanthrene desorption at 75 °C to desorption at 25 °C. These calculated scaling factors are shown in the last column of Table 2. The time scale for each desorption profile at 75 °C was then increased by the corresponding value of this factor to produce a predicted desorption profile at 25 °C. The predicted 25 °C desorption curves are compared to the measured 25 °C desorption data in Figure 3A−C. Dashed lines in the figures denote ± one standard deviation from the predictions based on propagation of uncertainties in $E_{app,d}$. Statistical confidence regions are wide because $E_{app,d}$ for each sample is based upon only three desorption rate experiments. Statistical confidence regions can be compressed by performing a larger number of experiments at additional temperatures.

It is important to note that the predicted desorption profiles for 25 °C were generated independently of the data points in the figures. It is rather remarkable that the desorption predictions agree so well with measured data in all cases even though the phenanthrene desorption rates themselves vary by orders of magnitude for the six samples (Table 1). The 25 °C predictions matched the measured desorption data to within approximately 3%, 10%, and 20%, respectively, for Lachine shale, Chelsea soil, and Wagner soil. Furthermore, each predicted profile was generated with only 2−3 days of laboratory experimental effort, while the actual measurements at 25 °C required 250−640 days. Because the desorption profiles at the higher temperatures so well match the extended profiles determined at 25 °C, it is clear that the rapid superheated water technique captures the behavior of even the highly desorption resistant fractions of sorbed contaminant.

Summation of Methodologies. The technique for rapid superheated water prediction of long-term desorption behavior described in this paper can be summarized briefly as follows: (i) rates of solute desorption from contaminated sorbents are measured at elevated temperatures; (ii) each high-temperature desorption rate curve is simulated using an appropriate desorption model (the biphasic first-order model was used in the present work) to determine a rate constant (e.g., k_s) for the slowly desorbing HOC fraction at each temperature; (iii) the data are modeled by the Arrhenius equation to determine apparent activation energies for the desorption process; (iv) apparent activation energies are used to calculate ratios of HOC desorption rate constant values measured at higher temperatures to those at the ambient temperatures of interest (i.e., temporal scaling factors) using the Arrhenius relationship; and (v) these temporal scaling factors are then used to expand the time scales of the desorption profiles measured at higher temperatures to obtain the profiles to be expected at corresponding ambient temperatures.

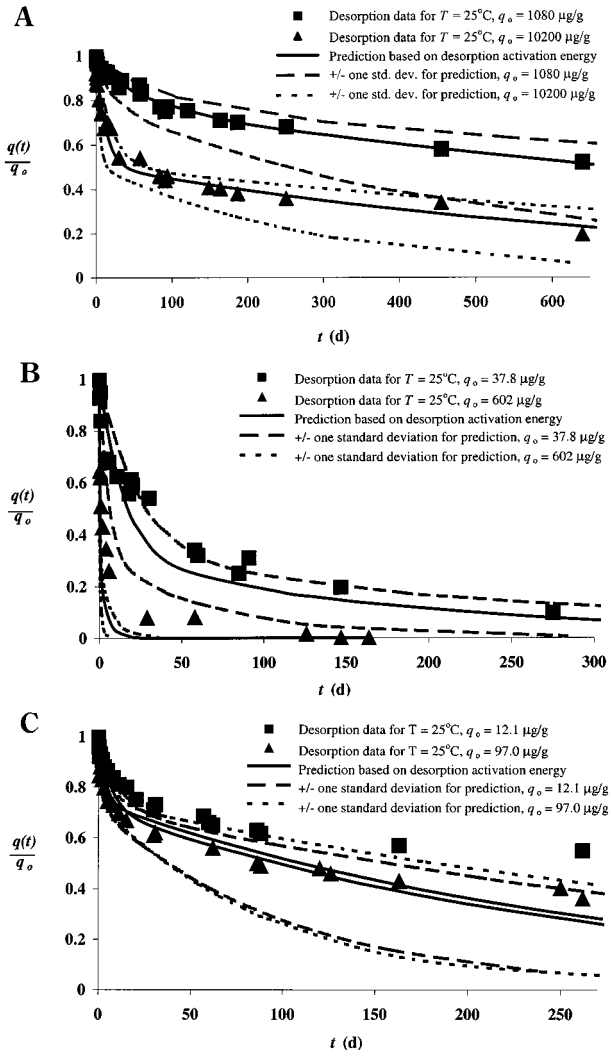

FIGURE 3. Comparisons of predicted 25 °C desorption rate profiles and measured data for (A) Lachine shale, (B) Chelsea soil, and (C) Wagner soil.

Effects of Superheated Water on Sorbents. A previous paper reported that partial extraction of soil organic matter with subcritical water at 250 °C permanently altered the sorptive reactivity of Chelsea soil for phenanthrene, attributing this to diagenesis-like changes to the soil's residual organic matter (*40*). This raises a question as to whether the desorption experiments conducted at temperatures of up to 150 °C in this work permanently altered the geosorbent SOMs. If so, correlations between 25 °C desorption and higher temperature desorption would be inappropriate. To assess this possibility, we treated uncontaminated Chelsea, Wagner, and Lachine sorbents using a range of superheated water temperatures and retained the treated samples for subsequent isotherm measurements. Samples of each sorbent were exposed to a 1.0 mL/min flow of superheated water for 3 h at 150, 175, 200, and 250 °C in the dynamic system described earlier. Pressure was elevated to a level high enough to maintain liquid aqueous phases during the superheated water treatments. Table 3 lists Freundlich isotherm parameters for the original geosorbents and those treated with superheated water. Isotherms for the original and Chelsea samples are shown in Figure 4 along with Freundlich model fits to the data. The dramatic increase in sorption capacity of Chelsea soil after 250 °C water treatment has been discussed elsewhere (*40*). Of the three geosorbents studied here, the Chelsea soil

TABLE 3. Sorption Isotherm Parameters and Calculated Concentration-Dependent Distribution Coefficients for Original and Subcritical Water Extracted Geosorbents

	Freundlich sorption parameters				K_D (L/g)[c]	
sorbent	log K_F[a]	n	R^2	N[b]	$C_e = 10$ μg/L	$C_e = 100$ μg/L
Chelsea soil	0.612 ± 0.034[d]	0.724 ± 0.018	0.998	19	[2.07, 2.26][e]	[1.11, 1.19]
150 °C SW Chelsea	0.633 ± 0.068	0.730 ± 0.032	0.993	20	[2.12, 2.53]	[1.18, 1.29]
175 °C SW Chelsea	0.733 ± 0.057	0.718 ± 0.034	0.992	18	[2.60, 3.07]	[1.34, 1.62]
200 °C SW Chelsea	0.885 ± 0.048	0.705 ± 0.030	0.994	18	[3.62, 4.19]	[1.81, 2.16]
250 °C SW Chelsea	1.26 ± 0.053	0.676 ± 0.031	0.991	20	[8.15, 9.22]	[3.89, 4.35]
Wagner soil	−0.186 ± 0.178	0.787 ± 0.093	0.963	15	[0.316, 0.505]	[0.205, 0.291]
150 °C SW Wagner	−0.184 ± 0.105	0.803 ± 0.067	0.978	17	[0.359, 0.481]	[0.222, 0.315]
175 °C SW Wagner	−0.142 ± 0.094	0.835 ± 0.058	0.983	18	[0.433, 0.564]	[0.290, 0.395]
200 °C SW Wagner	−0.0205 ± 0.080	0.757 ± 0.049	0.985	18	[0.485, 0.613]	[0.272, 0.358]
250 °C SW Wagner	−0.343 ± 0.229	0.678 ± 0.116	0.925	15	[0.786, 1.40]	[0.417, 0.603]
Lachine shale	2.42 ± 0.062	0.563 ± 0.035	0.987	18	[88.3, 104]	[32.5, 37.6]
150 °C SW Lachine	2.36 ± 0.064	0.577 ± 0.037	0.986	18	[78.7, 93.7]	[29.7, 35.4]
175 °C SW Lachine	2.41 ± 0.071	0.570 ± 0.041	0.982	18	[86.8, 105]	[32.1, 39.3]
200 °C SW Lachine	2.39 ± 0.082	0.578 ± 0.050	0.976	18	[82.5, 103]	[31.1, 39.2]
250 °C SW Lachine	2.74 ± 0.051	0.438 ± 0.026	0.991	14	[140, 160]	[38.9, 42.9]

[a] K_F has units of (μg/g)/(μg/L)^n. [b] Number of data points in isotherm. [c] Calculated using the listed Freundlich isotherm parameters, $K_D = q_e/C_e$. [d] 95% confidence intervals. [e] 95% confidence region.

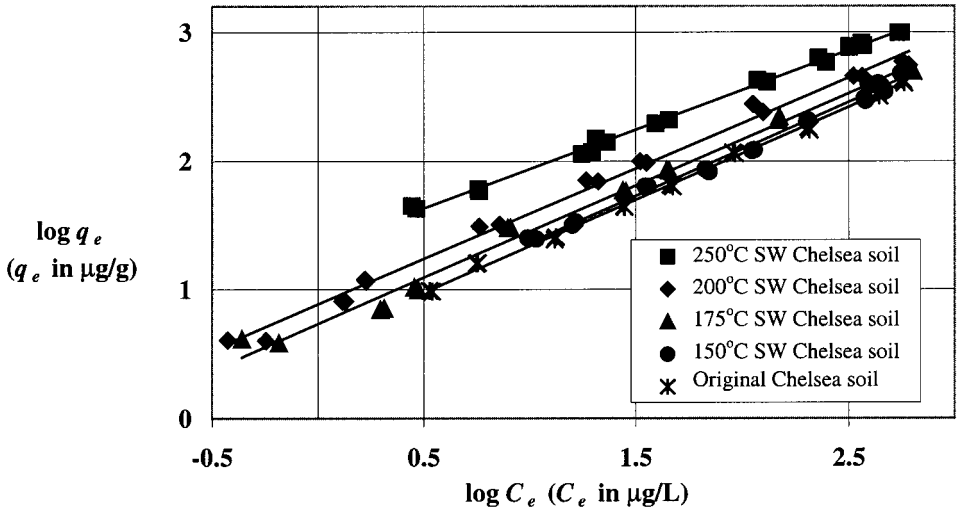

FIGURE 4. Effects of superheated water treatment of Chelsea soil on subsequent sorption isotherms.

contains the geologically youngest SOM and is therefore likely to be most markedly altered at elevated temperatures and pressures. Superheated water treatment causes changes in organic composition and functionality in a manner analogous to those of natural diagenesis processes. It is therefore not surprising that the Wagner soil and Lachine shale, because they contain principally geologically mature kerogen, are less affected in their properties and behaviors by high temperature and pressure.

For purposes of rapid comparison of results, the last two columns in the table list 95% confidence regions for concentration-dependent solute distribution coefficients calculated at 10 and 100 μg/L aqueous phase equilibrium concentrations. The data reveal that the superheated water treatment did not cause statistically significant changes in the sorptive reactivity of Chelsea soil at temperatures ≤150 °C nor in those of the Wagner soil and Lachine shale at temperatures ≤200 °C. Because the phenanthrene desorptions were all conducted at temperatures less than or equal to 150 °C, we conclude that geosorbent organic matter was not permanantly altered in the experimental process described. Desorption isotherms measured for selected samples additionally revealed that desorption hysteresis was not introduced for Chelsea soil treated at temperatures up to 150 °C and that the normal hysteresis observed for Lachine shale was not changed by treatment temperatures as high as 200 °C.

While the analyses described above suggest that there were no significant permanent changes to soil organic matter at the temperature employed, they do not rule out the possibility of temporary changes. However, as noted previously, when the 25 °C desorption rate constants are included in the Arrhenius plot, there is a strong linear relationship between $\ln(k_s)$ and T^{-1}. Thus, even if the higher temperatures might have caused temporary reversible changes to the soil organic matter, the desorption process activation energy remained essentially constant over this temperature range. Furthermore, the time-scaled desorption profiles at 25 °C matched those at temperatures of up to 150 °C for all samples. Thus, although the soil organic matter of at least the Chelsea soil might have been in a somewhat less rigid state at the elevated temperatures, desorption was still biphasic, with the slowly desorbing fraction having an apparent first-order rate constant about 2 orders of magnitude lower than that for the rapidly desorbing fraction.

In summary, an experimental methodology employing superheated water desorption has been developed for predicting long-term contaminant release rates from soils and sediments as well as the desorption-resistant fractions of the total contaminant burdens of such materials. The

technique has great potential practical value because contaminant desorption experiments at ambient temperatures commonly require months or years, while the superheated water desorptions used to develop activation energies for predictions of ambient temperature behavior can be completed in a matter of hours or days. We expect the technique to be applicable to other hydrophobic sorbates beside the phenanthrene tested here and to field-contaminated samples as well, but further experimental work is needed to verify this hypothesis.

Acknowledgments

We thank Tom Yavaraski and Dr. Hong Fang for their invaluable assistance in the experimental phases of this work, and Dr. Pierre Goovaerts for his advice on numerical methods for modeling the experimental data. Funding for the research was provided by the Great Lakes and Mid-Atlantic Center for Hazardous Substance Research under a grant from the Office of Research and Development, U.S. Environmental Protection Agency. Partial funding of the research activities of the Center was also provided by the State of Michigan Department of Environmental Quality. The content of this publication does not necessarily represent the views of either agency. Partial support was also provided in the form of an EPA Science To Achieve Results graduate environmental education fellowship award to M.D.J.

Literature Cited

(1) Coates, J. T. *J. Contam. Hydrol.* **1986**, *1*, 191−210.
(2) Carroll, K. M.; Harkness, M. R.; Bracco, A. A.; Balcarcel, R. R. *Environ. Sci. Technol.* **1994**, *28*, 253−258.
(3) Pignatello, J. J.; Ferrandino, F. J.; Huang, L. Q. *Environ. Sci. Technol.* **1993**, *27*, 1563−1571.
(4) Scribner, S. L.; Benzing, T. R.; Sun, S. B.; Boyd, S. A. *J. Environ. Qual.* **1992**, *21*, 115−120.
(5) Steinberg, S. M.; Pignatello, J. J.; Sawhney, B. L. *Environ. Sci. Technol.* **1987**, *21*, 1201−1208.
(6) White, J. C.; Hunter, M.; Nam, K. P.; Pignatello, J. J.; Alexander, M. *Environ. Toxicol. Chem.* **1999**, *18*, 1720−1727.
(7) Scow, K. M.; Hutson, J. *Soil Sci. Soc. Am. J.* **1992**, *56*, 119−127.
(8) Nam, K.; Alexander, M. *Environ. Sci. Technol.* **1998**, *32*, 71−74.
(9) Lueking, A. D.; Huang, W. L.; Soderstrom-Schwarz, S.; Kim, M. S.; Weber, W. J., Jr. *J. Environ. Qual.* **2000**, *29*, 317−323.
(10) Allen-King, R. M.; Groenevelt, H.; Warren, C. J.; Mackay, D. M. *J. Contam. Hydrol.* **1996**, *22*, 203−221.
(11) Alexander, M. *Environ. Sci. Technol.* **1995**, *29*, 2713−2717.
(12) Tang, J. X.; Alexander, M. *Environ. Toxicol. Chem.* **1999**, *18*, 2711−2714.
(13) Chung, N.; Alexander, M. *Environ. Sci. Technol.* **1999**, *33*, 3603−3606.
(14) Chung, N. H.; Alexander, M. *Environ. Sci. Technol.* **1998**, *32*, 855−860.
(15) Hatzinger, P. B.; Alexander, M. *Environ. Sci. Technol.* **1995**, *29*, 537−545.
(16) Kelsey, J. W.; Kottler, B. D.; Alexander, M. *Environ. Sci. Technol.* **1997**, *31*, 214−217.
(17) Cornelissen, G.; Rigterink, H.; Ferdinandy, M. M. A.; Van Noort, P. C. M. *Environ. Sci. Technol.* **1998**, *32*, 966−970.
(18) Hawthorne, S. B.; Bjorklund, E.; Bowadt, S.; Mathiasson, L. *Environ. Sci. Technol.* **1999**, *33*, 3152−3159.
(19) Weber, W. J., Jr.; Young, T. M. *Environ. Sci. Technol.* **1997**, *31*, 1686−1691.
(20) Young, T. M.; Weber, W. J., Jr. *Environ. Sci. Technol.* **1997**, *31*, 1692−1696.
(21) Young, T. M.; Weber, W. J., Jr. *Environ. Sci. Technol.* **1995**, *29*, 92−97.
(22) Brusseau, M. L. *Environ. Sci. Technol.* **1991**, *25*, 134−142.
(23) Nkedi-Kizza, P.; Brusseau, M. L.; Rao, P. S. C.; Hornsby, A. G. *Environ. Sci. Technol.* **1989**, *23*, 814−820.
(24) Arocha, M. A.; Jackman, A. P.; McCoy, B. J. *Environ. Sci. Technol.* **1996**, *30*, 1500−1507.
(25) Ball, W. P.; Roberts, P. V. *Environ. Sci. Technol.* **1991**, *25*, 1237−1249.
(26) Cornelissen, G.; van Noort, P. C. M.; Govers, H. A. J. *Environ. Sci. Technol.* **1998**, *32*, 3124−3131.
(27) Grathwohl, P.; Reinhard, M. *Environ. Sci. Technol.* **1993**, *27*, 2360−2366.
(28) Harmon, T. C.; Roberts, P. V. *Environ. Prog.* **1994**, *13*, 1−8.
(29) Werth, C. J.; Reinhard, M. *Environ. Sci. Technol.* **1997**, *31*, 697−703.
(30) Wu, S. C.; Gschwend, P. M. *Environ. Sci. Technol.* **1986**, *20*, 717−725.
(31) Veith, W. R. *Diffusion in and Through Polymers: Principles and Applications*; Oxford University Press: New York, 1991.
(32) Rogers, C. E. *The physics and chemistry of the organic solid state*; Interscience Publishers: New York, 1965; Vol. 2.
(33) Pignatello, J. J.; Xing, B. S. *Environ. Sci. Technol.* **1996**, *30*, 1−11.
(34) Xing, B. S.; Pignatello, J. J. *Environ. Sci. Technol.* **1997**, *31*, 792−799.
(35) Farrell, J.; Reinhard, M. *Environ. Sci. Technol.* **1994**, *28*, 63−72.
(36) Farrell, J.; Grassian, D.; Jones, M. *Environ. Sci. Technol.* **1999**, *33*, 1237−1243.
(37) Cornelissen, G. *Environ. Sci. Technol.* **1997**, *31*, 454−460.
(38) Durand, B. *Kerogen: Insoluble Organic Matter from Sedimentary Rocks*; Techip: Paris, 1980.
(39) Tissot, B. P.; Welte, D. H. *Petroleum Formation and Occurrence*; Springer-Verlag: New York, 1984.
(40) Johnson, M. D.; Huang, W. L.; Dang, Z.; Weber, W. J., Jr. *Environ. Sci. Technol.* **1999**, *33*, 1657−1663.
(41) Huang, W. L.; Young, T. M.; Schlautman, M. A.; Yu, H.; Weber, W. J., Jr. *Environ. Sci. Technol.* **1997**, *31*, 1703−1710.
(42) Huang, W. L.; Weber, W. J., Jr. *Environ. Sci. Technol.* **1997**, *31*, 2562−2569.
(43) Huang, W. L.; Weber, W. J., Jr. *Environ. Sci. Technol.* **1998**, *32*, 2, 3549−3555.
(44) Weber, W. J., Jr.; McGinley, P. M.; Katz, L. E. *Environ. Sci. Technol.* **1992**, *26*, 1955−1962.
(45) McGinley, P. M.; Katz, L. E.; Weber, W. J., Jr. *Environ. Sci. Technol.* **1993**, *27*, 1524−1531.
(46) Weber, W. J., Jr.; Huang, W. L. *Environ. Sci. Technol.* **1996**, *30*, 3130−3131.
(47) MacKay, D. M.; Shiu, W. Y. *J. Chem. Eng. Data* **1977**, *22*, 399−402.
(48) Hawthorne, S. B.; Yang, Y.; Miller, D. J. *Anal. Chem.* **1994**, *66*, 2912−2920.
(49) Pedit, J. A.; Miller, C. T. *Environ. Sci. Technol.* **1994**, *28*, 2094−2104.
(50) Cornelissen, G.; van Noort, P. C. M.; Govers, H. A. J. *Environ. Toxicol. Chem.* **1997**, *16*, 1351−1357.
(51) Karickhoff, S. W.; Morris, K. R. *Environ. Toxicol. Chem.* **1985**, *4*, 469−479.
(52) Cornelissen, G.; van Zuilen, H.; van Noort, P. C. M. *Chemosphere* **1999**, *38*, 2369−2380.
(53) Ten Hulscher, T. E. M.; Vrind, B. A.; Van den Heuvel, H.; Van der Velde, L. E.; Van Noort, P. C. M.; Beurskens, J. E. M.; Govers, H. A. J. *Environ. Sci. Technol.* **1999**, *33*, 126−132.
(54) Johnson, M. D., Keinath, T. M., II; Weber, W. J., Jr. *Environ. Sci. Technol.*, submitted for publication.
(55) Weber, W. J., Jr.; DiGiano, F. A. *Process Dynamics in Environmental Systems*; Wiley-Interscience: New York, 1996.
(56) Pignatello, J. J. *Environ. Toxicol. Chem.* **1990**, *9*, 1117−1126.
(57) Ten Hulscher, T. E. M. *Chemosphere* **1996**, *32*, 609−626.
(58) Crank, J., Park, G. S., Eds. *Diffusion in Polymers*; Academic Press: New York, 1968.
(59) Chihara, K.; Suzuki, M.; Kawazoe, K. *AICHE J.* **1978**, *24*, 237−246.
(60) Awum, F.; Narayan, S.; Ruthven, D. *Ind. Eng. Chem. Res.* **1988**, *27*, 1510−1515.
(61) Karger, J.; Ruthven, D. M. *Diffusion in Zeolites and Other Microporous Solids*; John Wiley and Sons: New York, 1991.
(62) Leboeuf, E. J.; Weber, W. J., Jr. *Environ. Sci. Technol.* **1997**, *31*, 1697−1702.

Received for review June 16, 2000. Revised manuscript received October 31, 2000. Accepted November 7, 2000.

ES001392C